

Hybrid Effect at Fiber Breaks in Twisted Blended Yarns

JOHN N. ROSSETTOS

*Department of Mechanical, Industrial & Manufacturing Engineering, Northeastern University,
Boston, Massachusetts 02115, U.S.A.*

THOMAS A. GODFREY

Natick Soldier Center, U.S. Army Soldier & Biological Chemical Command, Natick, Massachusetts 01760, U.S.A.

ABSTRACT

A previously developed micromechanical model is used to formulate the problem of a blended yarn, consisting of low elongation (LE) and high elongation (HE) fibers undergoing axial extension, with a fiber break in the central region of the hybrid fiber array. A hybrid parameter R , which is the ratio of the axial stiffness of the HE fibers to that of the LE fibers, is shown to have an important effect on the intact fiber stress concentration factor (SCF), and the broken fiber slip extent at the fiber break. While the SCF increases for HE fibers adjacent to broken LE fibers, it decreases for LE fibers adjacent to broken HE fibers as R takes on values away from unity (homogeneous yarn). Higher loading can therefore be sustained by the LE fibers, and a beneficial hybrid effect can be realized.

Blended or hybrid yarns, which consist of more than one kind of fiber, have been produced to develop improved strength and stiffness over what can be achieved in homogeneous yarns. This so-called hybrid effect has been observed in hybrid composite sheets [2, 14], indicating how higher loading and elongation can be sustained by high modulus (low elongation, LE) fibers than when they exist alone in a nonhybrid composite. The same effect appears to be possible for blended yarns. This is corroborated by our current results, which show that the stress concentration factor (SCF) of an LE fiber next to a broken HE (high elongation) fiber decreases, while the SCF of an HE fiber next to a broken LE fiber increases with decreasing values of the hybrid parameter R , the ratio of the axial stiffness of the HE to that of the LE fibers. This has a positive effect for yarns where the principal fibers are particular LE fibers, which are selected to be stronger than the dispersed HE fibers. It suggests that if a reduction in the SCF of the principal LE fiber has a dominant effect on yarn strength compared with the increased SCF of the HE fiber (since the HE fiber has a larger failure strain), a hybrid effect can be realized.

Near a fiber break, the neighboring fibers will slip, and the slip extent plays a role similar to the yield zone in the matrix near a fiber break [14] in fiber composites. We will show here how the SCF decreases with larger slip extents, supporting the notion that a slip acts as a dissipative mechanism, similar to matrix yielding in fiber composites.

In general, twisted fibrous structures, including yarns, ropes, and cables, exhibit transverse compressive forces induced by the remote tension along the yarn axis. Each fiber executes a quasi-helical path through the yarn, so that a radially outwardly directed, distributed reaction force from underlying fiber layers balances the tension on the curved fiber. The compressive forces that occur permit load transfer between abutting fibers through friction and give the yarn cohesiveness. With increasing yarn tension, transverse compressive forces also increase, thereby increasing the magnitude of the frictional load transfer between fibers. This mechanism, first noted by Galileo [3], is particularly important in structures twisted from short plant and animal fibers (*i.e.*, staple yarns), which rely entirely on friction for structural integrity. The induced transverse compressive forces in our work are important in providing the frictional forces at slipping contact surfaces between LE and HE fibers near a fiber break.

In representative past work on yarn stress analysis, Hearle [7, pp. 175–212], Kilby [9], and Thwaites [15, 16] treated a helical element of the twisted yarn, parallel to the local filament direction, as a continuum with a variety of simplifying assumptions for the constitutive behavior of the packed fibers. As such, the main concern is with deformations that may be considered homogeneous over large number of fibers, and so no attention is given to problems of broken fibers. However, the results for yarn internal stresses obtained in these studies motivated our

model used for frictional load transfer at slipping fiber contact surfaces in the analytical treatment of broken fibers (Godfrey and Rossetto [5]). There, we showed how broken LE fiber fragments continue to contribute to the load-carrying ability of the fiber array [5]. Our focus here, however, will be on the stress concentration (SCF) near a fiber break, which not only gives load sharing (by adjacent fibers) information used in strength prediction, but provides a means of evaluating the hybrid effect.

Past work on strength prediction has emphasized the stochastic aspects of the failure process, from the early work of Daniels [1] to representative recent work by Phoenix [11], Pitt and Phoenix [12], and Realf *et al.* [13], who provided a particularly important contribution to the failure of blended yarns. We discussed these works and related literature involving statistical theories for the mechanical behavior of fibrous composites in earlier work [5], so we will not pursue this topic here.

In this paper, we formulated a micromechanical model for a blended yarn consisting of LE and HE fibers undergoing axial extension, with a fiber break in the central region of the hybrid fiber array. The configuration of the fiber array contains the same number of HE and LE fibers. We show that the stress concentration in the fiber adjacent to the break will depend, in an important way, on whether the broken fiber is HE or LE. The analysis of frictional slip forces acting in the slip region in fibers near the break is motivated by results for yarn internal stresses [7, pp. 175–212]. The model we develop in this paper has a mathematical structure similar to Hedgepeth and Van Dyke's [8] shear-lag model for a three-dimensional fiber composite. In the composite case, load transfer takes place by shear of the matrix phase. For packed fiber arrays in hybrid yarns, load transfer occurs through geometric changes in the fibers and surface friction. The model leads to a system of second-order differential equations, which we have solved by an eigenvector expansion approach [4, 5]. We obtain solutions in each of two regions, a region where slip occurs between fibers and one where there is no slip. We then apply appropriate continuity and boundary conditions in the cases considered.

Analysis

MICROMECHANICAL MODEL

In our model of a twisted yarn, which is assumed to have a well accepted idealized helical structure [7], the fibers follow helical paths and lie in co-axial concentric layers. In the central region of the yarn, however, the fibers are nearly parallel to the yarn axis, and they experience the highest strains during yarn extension.

Since rupture usually starts in the central region, we base our model in this region.

Previously, we indicated [5] that square packing provides an effective model for real fiber packed within yarns. Therefore, near the yarn's center, the microstructure is represented by a square-stacked mixed array of parallel, linearly elastic fibers. Also, our model assumes roughly similar cross-sectional dimensions for HE and LE fibers, to the extent that approximately square packing can be achieved.

We derive the equations of our model by considering an equal number of HE and LE fibers. A typical finite array is shown in Figure 1. The fibers are numbered (n, m) , where n is the column number and m is the row number. In Figure 1, the shaded fibers are LE and the blank fibers are HE. The center fiber $(0, 0)$ in Figure 1 is an HE fiber and will be considered broken in the development to follow. The array is extended in the x -direction to a strain ϵ . It is convenient to take as the displacement reference the position of points on an undamaged fiber array under the same strain. Note also that the square region in Figure 1 exhibits eight-fold symmetry, and this will reduce the number of equations needed in the analysis.

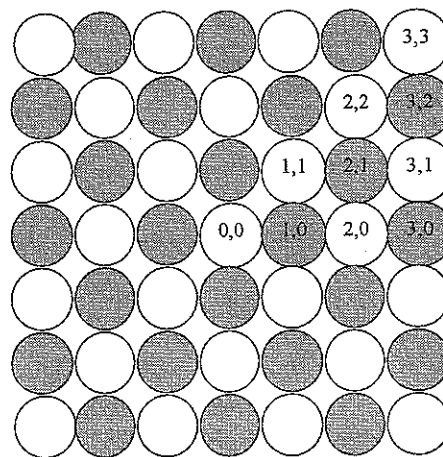


FIGURE 1. Numbering scheme for finite section of fiber array; LE fiber shown shaded.

NO SLIP BETWEEN FIBERS

The general form of the equilibrium equation for an (n, m) fiber can be derived as follows (see unit cell in Figure 2a): For equilibrium, it is necessary to consider the shear forces (surface friction between fibers) acting on the (n, m) fiber from its four abutting fibers in Figure 2. Accordingly, we define "shear flow" as the shear force per unit length, and assume [5] it is proportional to the difference in the displacement of the two abutting fibers.

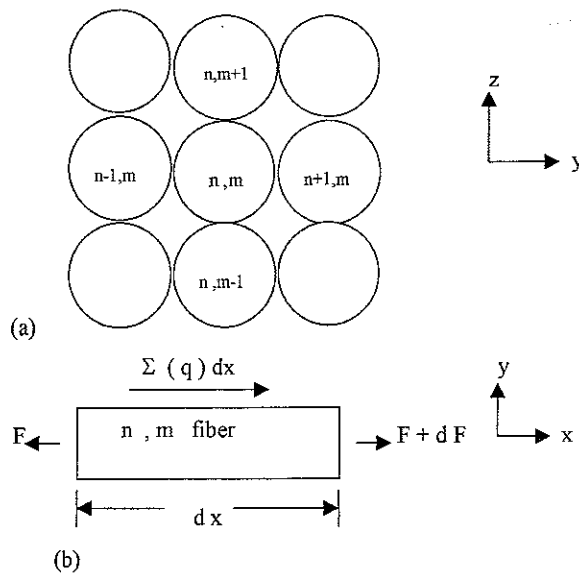


FIGURE 2. (a) n, m th fiber and abutters, (b) n, m th fiber equilibrium.

For instance, the shear flow $q_{n,n+1}^m$ caused by the $(n + 1, m)$ fiber on the (n, m) th fiber is taken as

$$q_{n,n+1}^m = k(u_{n+1,m} - u_{n,m}) \quad (1)$$

In the shear flow notation, superscripts denote row numbers and subscripts denote column numbers. Also, the displacement pattern is taken so that the shear forces on the (n, m) fiber by the $(n + 1, m)$ and $(n, m + 1)$ fibers in Figure 2a are in the positive x -direction, while the forces on the (n, m) fiber by the $(n - 1, m)$ and $(n, m - 1)$ fibers are in the negative x -direction. We use notation where E^*A^* and EA are the effective axial stiffness of the HE and LE fibers, respectively. Introduce $u_{n,m}$ as the axial (x -direction) displacement of fiber (n, m) at position x . If (n, m) is an HE fiber, then in Figure 2b, $dF = E^*A^*(d^2u_{n,m}/dx^2)dx$. Also, Σq involves four terms that can be written in terms of displacements using Equation 1. Equilibrium for fiber (n, m) can then be written as

$$E^*A^* \frac{d^2u_{n,m}}{dx^2} + k(u_{n+1,m} - u_{n,m}) - k(u_{n,m} - u_{n-1,m}) + k(u_{n,m+1} - u_{n,m}) - k(u_{n,m} - u_{n,m-1}) = 0 \quad (2)$$

Nondimensional quantities ξ and $U_{n,m}$ are defined by

$$x = \sqrt{E^*A^*/k}\xi, \quad u_{n,m} = \epsilon \sqrt{E^*A^*/k}U_{n,m} \quad (3)$$

Equation 2 can then be written as

$$U_{n,m}'' + (U_{n+1,m} + U_{n-1,m} + U_{n,m+1} + U_{n,m-1} - 4U_{n,m}) = 0 \quad (4)$$

where primes denote differentiation with respect to ξ . It is instructive to write equations for fibers $(0, 0)$, $(1, 0)$, and $(1, 1)$. Using Equation 4 to write the equation for fiber $(0, 0)$ and noting the symmetry in Figure 1, where $U_{0,1} = U_{1,0} = U_{-1,0} = U_{0,-1}$, we write

$$U_{0,0}'' + 4(U_{1,0} - U_{0,0}) = 0 \quad (5)$$

In a similar fashion, we obtain the equation for fiber $(1, 1)$ from Equation 4 by noting that $U_{1,2} = U_{2,1}$ and $U_{0,1} = U_{1,0}$, which gives

$$U_{1,1}'' + (2U_{2,1} + 2U_{1,0} - 4U_{1,1}) = 0 \quad (6)$$

Since fiber $(1, 0)$ is an LE fiber, its equation takes on a slightly different form than Equation 4. Its equilibrium equation (using $u_{1,-1} = u_{1,1}$ from symmetry) is given by

$$EA d^2u_{1,0}/dx^2 + ku_{2,0} - 4ku_{1,0} + k_{0,0} + 2ku_{1,1} = 0 \quad (7)$$

Using Equation 3, we can write Equation 7 in a nondimensional form as

$$U_{1,0}'' + R(U_{2,0} + 2U_{1,1} + U_{0,0} - 4U_{1,0}) = 0 \quad (8)$$

where $R = E^*A^*/EA$. The parameter R (the ratio of HE to LE fiber axial stiffness) has been used in the hybrid composite literature [2, 14] and plays an important role in our paper. R is equal to 1 for nonhybrids and takes on fractional values in the range $1/6 \leq R \leq 1$ for blended (hybrid) yarns.

FRICIONAL SLIP OF BROKEN FIBERS

Assume slip occurs between the broken HE fiber and the abutting LE fibers (Figure 1) near the break in the region $0 \leq x < a$. For the HE fiber $(0, 0)$, equilibrium gives

$$E^*A^* d^2u_{0,0}/dx^2 - 4q_s = 0 \quad (9)$$

where q_s is the shear flow (shear/unit length) along the contact line. If we define a shear parameter Q by

$$Q = \frac{q_s}{\epsilon \sqrt{kE^*A^*}} \quad (10)$$

and use Equation 3, Equation 9 becomes

$$U_{0,0}'' - 4Q = 0 \quad (11)$$

For the LE fiber $(1, 0)$, slip occurs along the contact line with the HE fiber $(0, 0)$, but there is no slip between it and the other three abutters. Writing the equilibrium equation and using symmetry, so $U_{1,-1} = U_{1,1}$, we can derive the nondimensional equation as

$$U_{1,0}'' + R(U_{2,0} - 3U_{1,0} + 2U_{1,1}) + RQ = 0 \quad (12)$$

For the HE fiber (1, 1), there are no slip surfaces, so equilibrium gives an equation identical to Equation 6.

In earlier work [5], we developed an expression for the shear flow q_s , where we assumed (a fairly good approximation of) equal radial and circumferential stress components for most of the yarn interior. We assumed that the lateral "hydrostatic" stress σ experienced by the fiber is the product of the axial stress in the fiber array σ_x and a function η of the yarn surface helix angle and the radial position of the fiber array within the yarn. Thus, the lateral stress is given by $\sigma = -\bar{E}\epsilon\eta$, where \bar{E} is the axial stiffness of the fiber array. Denoting the average fiber spacing as d , Adminton's law requires that $q_s = -\mu d\sigma$, where μ is the coefficient of friction between slipping fiber surfaces, so that q_s is written as $q_s = \mu d\bar{E}\epsilon\eta$.

It is reasonable to expect that q_s should increase with strain, with the particular increase leveling off as the yarn approaches a taut condition. This effect can be represented in the analysis by assuming that μ varies as μ_0/ϵ^n , so that the shear flow q_s can be written as

$$q_s = \mu_0 d \bar{E} \epsilon^{1-n} \eta \quad (13)$$

where μ_0 is a constant and the friction index n can take on fractional values. We use values of n ranging from 0.5 to 0.9 in these results, and the principal conclusions of this paper about the hybrid effect are not affected for such variations in n . We next define a nondimensional shear flow by $\bar{q}_s = q_s/\mu_0 d \bar{E} \eta$. When plotted against strain ϵ , the quantity \bar{q}_s , as indicated in Figure 3, approaches (asymptotic) taut condition values more steeply when $n = 0.9$ than say when $n = 0.5$ for example. Values of n at the higher end ($n = 0.9$) represent stiffer yarns where tautness occurs at lower strains. Values of n at the lower end ($n = 0.5$) represent more flexible yarns. As we will show, our results for the stress concentration factor are in qualitative agreement with those for hybrid fiber composite sheets [14], where the frictional slip zone in the yarn for our case, and the plastic yield zone in the matrix of the fiber composite sheet, play similar roles.

NONDIMENSIONAL FIBER LOADS

We denote by $p_{n,m}$ and $p_{n,m}^*$, the change in loads in the LE and HE fibers, respectively, due to a fiber break. Far from the break, these loads are denoted by p and p^* , respectively. Dimensionless loads $P_{n,m}$ and $P_{n,m}^*$ are then defined by

$$(p_{n,m}, p_{n,m}^*) = p^*(P_{n,m}, P_{n,m}^*) \quad (14)$$

We assume a uniform strain far from the break (at $x = \infty$), so that the strain there can be written as $\epsilon = p^*/E^*A^* = p/EA$. The total load in, say, the HE fiber adjacent to the break is then given by $p^* + p_{n,m}^*$, where

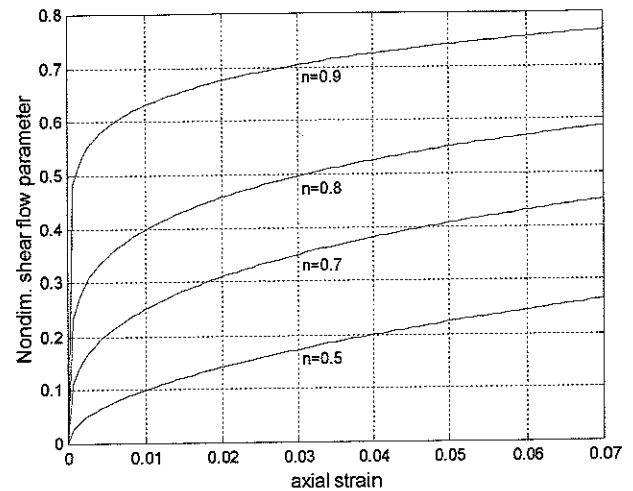


FIGURE 3. Shear flow parameter \bar{q}_s versus axial strain ϵ for various values of friction index n .

p^* is the reference load before the break. Noting that $P_{n,m}^* = E^*A^* du_{n,m}^*/dx$, and using Equations 3 and 14, the total nondimensional load for the HE fiber can be written as

$$P_{n,m}^* = 1 + U'_{n,m} \quad (15)$$

Note that, by definition, $P_{n,m}^* = p_{n,m}^*/p^*$ is, in fact, the stress concentration factor (SCF). Because of the assumption of uniform strain far from the break, we obtain the same expression as the right-hand side of Equation 15 for the SCF of an LE (n, m) fiber adjacent to an HE fiber break. In earlier work [6], we derived a similar equation with regard to damage growth in stressed fabrics.

With the expression for q_s given by Equation 13 and noting that the strain $\epsilon = p/EA$, the quantity Q in Equation 10 can be written as

$$Q = \frac{\mu_0 d \bar{E} \eta (EA)^n}{p^n \sqrt{kE^*A^*}} \quad (16)$$

BOUNDARY VALUE PROBLEM

Because of the eight-fold symmetry in the square region unit cell of fibers lying in the rows and columns numbered $-M$ through M , we need only write equations for fibers in a right triangular wedge. This is shown in Figure 1 for the case $M = 3$. For a sufficiently large M [5], we assume that the outer boundary of the square region is free of any shear flows arising from interactions with fibers lying in the $M + 1$ and $M - 1$ row or column. It turns out that choosing $M = 2$ or 4 makes a negligible difference in the results, indicating that the significant deformations occur near the broken fiber.

Although we derived equations here for only the center HE fiber (0, 0) and its neighboring fibers (1, 0) and (1, 1)—Equations 5, 6, 8, 11, 12—we can develop the equations for the remaining fibers in the wedge region in a similar and straightforward manner.

Slip will occur between the broken HE fiber (0, 0) and its LE abutters (Figure 1) in a region $0 \leq x < a$, where a is the extent of the slip region. The corresponding dimensionless slip region extent is denoted by α , where $a = \sqrt{E^*A^*/k\alpha}$, using Equation 3. The unit cell is divided into region I, $0 \leq \xi < \alpha$, where slip occurs, and region II, $\alpha \leq \xi$, where no slip occurs. The system of equations in region I consists of Equations 11, 12, and 4, specialized as needed for each of the remaining fibers in the wedge. In region II, the system of equations includes Equations 5, 8, and 4, specialized as needed for each of the remaining fibers in the wedge.

The general boundary conditions and continuity conditions to be applied are given as shown below. Since the system of equations contains constant coefficients, the general solution for the nondimensional displacements will include both positive and negative exponentials.

In region I, at $x = 0$, fiber (0, 0) is stress free (broken) so that $P_{0,0}^* = 0$. Using Equation 15, this gives

$$U'_{0,0} = -1 \quad (17)$$

We showed similar boundary condition in more detail in earlier work [6]. For the intact fibers, $\xi = 0$ is also a plane of symmetry, so that

$$U_{n,m}(0) = 0, \quad (n, m) \neq (0, 0) \quad (18)$$

In region II where $\xi > \alpha$, we must drop positive exponentials to satisfy conditions at $\xi = \infty$ (i.e., far from the break). Since all fibers are continuous at $\xi = \alpha$, the following continuity conditions hold, where superscripts I and II refer to solutions in regions I and II, respectively:

$$U_{n,m}^I(\alpha) = U_{n,m}^{II}(\alpha), \quad U'_{n,m}^I(\alpha) = U'_{n,m}^{II}(\alpha) \quad (19)$$

An additional condition arises from the assumption that slipping is approached in a continuous manner—the shear flows on the broken fiber in the nonslipping region approach those in the slipping region as $\xi \rightarrow \alpha$. Using Equations 5 and 11, we can write this condition

$$Q = [U_{0,0}^{II}(\alpha) - U_{1,0}^{II}(\alpha)] \quad (20)$$

The system of equations in regions I and II is written in matrix form, and solutions in each region are obtained using an eigenvector expansion technique, as described in detail for a similar boundary value problem in earlier work [4, 6]. We complete the solution process by selecting values of the slip region extent α (this defines the two regions) and determining the values of the integration constants and parameter Q , such that the boundary and

continuity conditions, Equations 17–20, are satisfied. Results for the stress concentration factor (SCF) and slip extent will be plotted against the parameter p/p_L , where p_L is the applied load far from the break that just starts slipping, and p is the corresponding current load above that value. We can obtain the ratio p/p_L from Equation 16, where Q is proportional to $1/p^n$ for fixed material and geometric properties. Therefore, we get

$$\frac{p}{p_L} = \left(\frac{Q_L}{Q} \right)^{1/n} \quad (21)$$

where Q_L is the corresponding value of Q when slipping just begins. Since we obtain the values of Q_L and Q as part of the solution process, we calculated p/p_L .

Results and Discussion

The nondimensional slip extent α is plotted against p/p_L in Figure 4 for the case where an HE fiber is broken. Note that p_L is the remote (far from break) fiber load that just initiates slipping, while p is the current load value above p_L . Curves are given for various values of the hybrid parameter R for a value of $n = 0.8$. When an LE fiber is broken, Figure 1 can still be used, but the shaded (LE) and blank (HE) fibers are now interchanged, so that the shaded (0, 0) LE fiber is broken. The relevant equilibrium equations for this case are developed accordingly, using the equilibrium concepts discussed earlier in the paper. The associated boundary value problem is solved in the same manner as for a broken HE fiber. In Figure 5, the slip extent α is plotted against p/p_L when an LE fiber is broken, for different R values and $n = 0.8$. Note in Figure 4 that the slip extent increases as R takes on values from 1 to $1/6$ when an HE fiber is broken, while

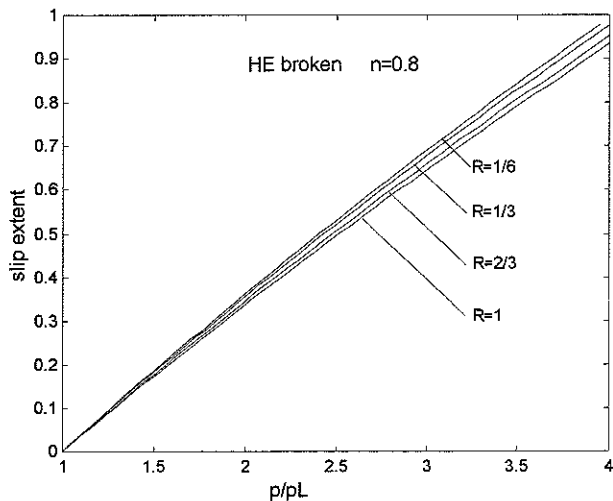


FIGURE 4. Slip extent α versus p/p_L ; HE fiber is broken, $n = 0.8$.

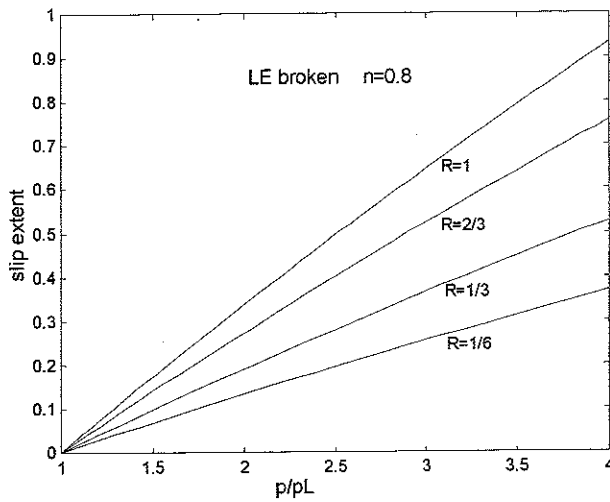


FIGURE 5. Slip extent α versus p/p_L ; LE fiber is broken, $n = 0.8$.

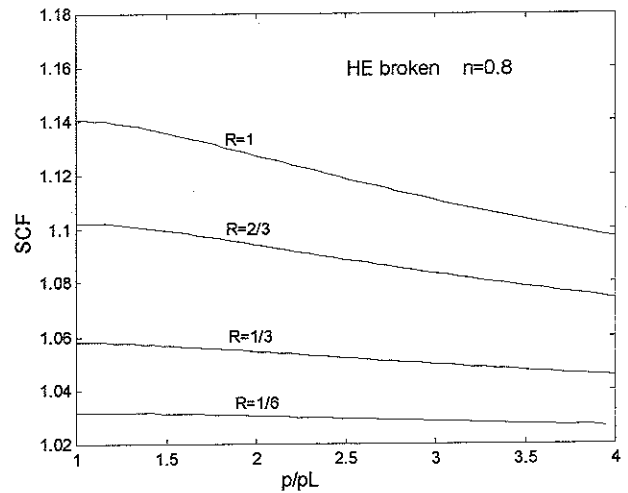


FIGURE 7. Stress concentration factor (SCF) versus p/p_L ; HE fiber is broken, $n = 0.8$.

it decreases (Figure 5) as R takes on values from 1 to $1/6$ when an LE fiber is broken. Recall that $R = E^*A/EA$, so that smaller values of R indicate greater differences in HE and LE fiber stiffness. If we regard slip as a dissipative mechanism, and observe that there is less slip when an LE fiber is broken (Figure 5), we should expect a larger stress concentration (SCF) near such a fiber break than for the case when an HE fiber is broken (Figure 4). This is borne out in Figure 6-8.

The stress concentration factor (SCF) is plotted against p/p_L in Figure 6 for the case when an LE fiber is broken and for a friction index value $n = 0.8$ for various values of R . It is clear that for a range of p/p_L values, SCF increases as R takes on values from 1 to $1/6$. For all values

of R , the SCF decreases with p/p_L . This is also expected, since the slip extent increases for all values of R with increasing p/p_L (Figure 5). We have indicated an analogous observation in earlier work [14] on composite sheets, where a matrix yield region in the composite plays a role similar to the slip region in our case. In Figure 7, the SCF is plotted against p/p_L when an HE fiber is broken. In this case, the SCF decreases as R goes from 1 to $1/6$. Note that the slip extent increases in this range as indicated in Figure 4.

In Figure 8, the SCF is plotted against the hybrid parameter R for various values of the friction index n . The load level is selected as $p/p_L = 2$, and the separate cases of HE and LE broken fibers are both shown. The

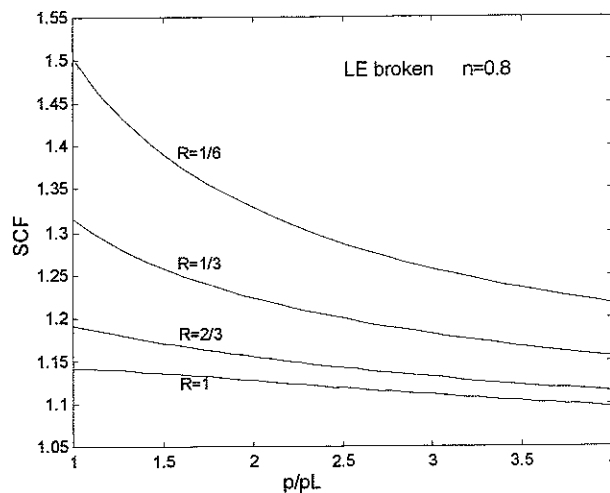


FIGURE 6. Stress concentration factor (SCF) versus p/p_L ; LE fiber is broken, $n = 0.8$.

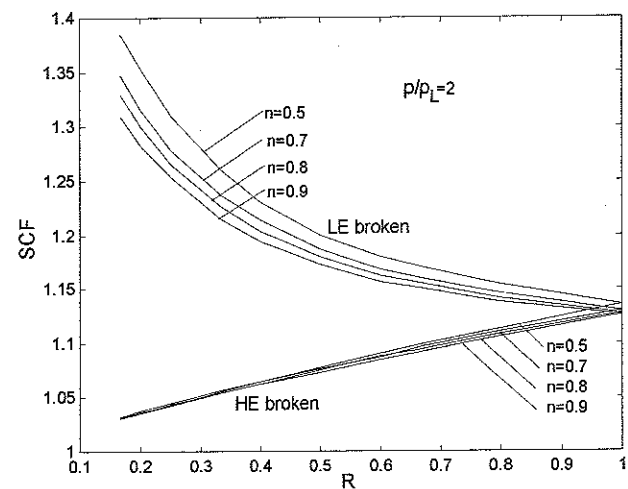


FIGURE 8. SCF versus R for various values of friction index n for the separate cases of HE and LE broken fibers. Load level, $p/p_L = 2$.

sensitivity of SCF to R is clearly indicated, with a more sharply increasing SCF for the case where an LE fiber is broken, and a mildly decreasing SCF in the case where an HE fiber is broken. As we see here, this trend is established for a range of n values from 0.5 to 0.9, so that the choice of n (for a given yarn) does not alter the fact that a hybrid effect is possible, where the principal fibers are LE fibers. Ultimately, differences in fiber strengths and failure statistics would both contribute to the exact nature of a given beneficial hybrid effect. Note also that for a given p/p_L , the SCF decreases as the friction index n increases. We can explain this by observing that for a given axial strain ϵ , the shear flow \bar{q}_s will increase with n as shown in Figure 3. This implies that for a larger n , a given slip region, with the larger shear (friction) forces developed, will take on more of the load of the broken fiber and hence lead to a smaller SCF. We can also interpret this as more energy dissipating in the slip region.

Conclusions

We have used a micromechanical model to develop the equations for deformation in a fiber array representing the microstructure of a blended (hybrid) yarn, consisting of an equal number of low elongation (LE) and high elongation (HE) fibers undergoing axial extension. We show in what manner the stress concentration (SCF) in the intact fiber next to a broken fiber depends on whether the broken fiber is an LE or an HE fiber. The SCF also depends, in an important way, on the parameter R , the ratio of HE to LE fiber stiffness. While SCF increases in an intact HE fiber when an LE fiber is broken, as R takes on values from 1 to $1/6$, it decreases for an intact LE fiber for the same range of R when an HE fiber is broken. A beneficial hybrid effect on yarn strength is therefore possible if the principal fibers are chosen as appropriate LE fibers. We also indicate how the slip region of a broken fiber and an associated friction index n play a role in this effect.

Literature Cited

1. Daniels, H. E., The Statistical Theory of Strength of Bundles of Threads, *Proc. R. Soc. Lond. A.* **183**, 405–435 (1945).

2. Fukuda, H., and Chou, T. W., Stress Concentrations in a Hybrid Composite Sheet, *J. Appl. Mech.* **50**, 845–848 (1983).
3. Galileo, Galilei, "Dialogues Concerning Two New Sciences," Leyden (1638), translated by A. De Salvio and A. Fabaro, Evanston, Illinois, 1914.
4. Godfrey, T. A., and Rossettos, J. N., The Onset of Tear Propagation at Slits in Stressed Uncoated Plain Weave Fabrics, *J. Appl. Mech.* **66**, 926–933 (1999).
5. Godfrey, T. A., and Rossettos, J. N., A Constitutive Model for Blended Yarn Extension with Fragmented Low-Elongation Fibers, *Textile Res. J.* **71**, 845–845 (2001).
6. Godfrey, T. A., and Rossettos, J. N., Damage Growth in Pre-stressed Plain Weave Fabrics, *Textile Res. J.* **68**, 359–370 (1998).
7. Hearle, J. W. S., Grosberg, P., and Backer, S., "Structural Mechanics of Fibers, Yarns, and Fabrics," Wiley-Interscience, NY, 1969.
8. Hedgepeth, J. M., and Van Dyke, P., Local Stress Concentrations in Imperfect Filamentary Composite Materials, *J. Compos. Mater.* **1**, 294–309 (1967).
9. Kilby, W. F., The Mechanical Properties of Twisted Continuous-Filament Yarns, *J. Textile Inst.* **55**, T589–T632 (1964).
10. Morton, W. E., and Hearle, J. W. S., "Physical Properties of Textile Fibers," Halsted Press, NY, 1975.
11. Phoenix, S. L., Statistical Theory for the Strength of Twisted Fiber Bundles with Applications to Yarns, *Textile Res. J.* **49**, 407–423 (1979).
12. Pitt, R. E., and Phoenix, S. L., On Modelling the Statistical Strength of Yarns and Cables Under Localized Load-Sharing Among Fibers, *Textile Res. J.* **51**, 408–425 (1981).
13. Realff, M. L., Pan, N., Seo, M., Boyce, M. C., and Backer, S. A., A Stochastic Simulation of the Failure Process and Ultimate Strength of Blended Continuous Yarns, *Textile Res. J.* **70** (5), 415–430 (2000).
14. Rossettos, J. N., and Olia, M., On the Hybrid Effect and Matrix Yielding at Fiber Breaks in Hybrid Composite Sheets, *Mech. Compos. Mat.* **2**, 275–280 (1995).
15. Thwaites, J. J., The Elastic Deformation of a Rod with Helical Anisotropy, *Int. J. Mech. Sci.* **19**, 161–168 (1976).
16. Thwaites, J. J., "Mechanics of Flexible Fibre Assemblies," Sijthoff & Noordhoff, Alphen aan den Rijn, The Netherlands, 1980, pp. 87–112.